Progress In Electromagnetics Research B, Vol. 13, 21–40, 2009

DISPERSION FLATTENED OPTICAL FIBER DESIGN FOR LARGE BANDWIDTH AND HIGH-SPEED OPTICAL COMMUNICATIONS USING OPTIMIZATION TECHNIQUE

S. Makoui

Photonics and Nanocrystals Research Lab. (PNRL)
Faculty of Electrical and Computer Engineering
University of Tabriz
Tabriz 51664, Iran

M. Savadi-Oskouei

National Iranian Gas Company
Tabriz, Iran

A. Rostami and Z. D. K. Kanani

Photonics and Nanocrystals Research Lab. (PNRL)
Faculty of Electrical and Computer Engineering
University of Tabriz
Tabriz 51664, Iran

Abstract—In this paper, design of the RII triple-clad structure as a dispersion flattened optical fiber including small pulse broadening factor as well as small dispersion and its slope applicable in broadband and fast communication is considered. The proposed optimization technique is based on the Genetic Algorithms (GA) consisting suitable fitness function for each application. The putting forward design method introduces the pulse broadening factor (σ/σ_0) about 1.0016 after 200 Km propagation at the zero dispersion wavelength that is so excellent compared to the structure (1.2794) reported in [2] recently. Meanwhile, the proposed structure provides high bit rate (more than 197.8 Gb/sec at 100 Km), large dispersion length (larger than 17400 Km), uniform dispersion slope ($[0.04, -0.08]$ ps/Km/nm^2) and broad bandwidths as well as small and uniform dispersion (smaller than 2.02 ps/Km/nm) at [1.55–1.7] μm wavelength interval

Corresponding author: M. Savadi-Oskouei (morteza_savadi79@yahoo.com).

even for core diameter larger than 4.62 μm. Another important thing discussed in this paper is a proposal for optimization of the broadening factor on large wavelength duration, which is necessary for large bandwidth applications. The suggested technique is capable to minimize the pulse broadening factor over duration of wavelengths that is necessary for large bandwidth applications such as dense wavelength division multiplexing (DWDM) and optical time division multiplexing (OTDM). Our calculation for extracting optical properties of the proposed structure is evaluated analytically. For this purpose modal analysis of these fibers for obtaining possible wave vectors for given system parameters are done using Transfer Matrix Method (TMM) in cylindrical coordinate.

1. INTRODUCTION

Recently high-speed and large bandwidth optical communications are basic demand in science and technology. High-speed data communication and computing is one of the serious requests for real time processing. Optical fiber based communication is the excellent alternative for these purposes which needs low dispersion as well as dispersion slope and large bandwidth supported by optical physical medium. Nowadays, applications such as time division multiplexing (OTDM) and dense wavelength division multiplexing (DWDM) are usual tasks in industry. Therefore by considering these applications, providing a large bandwidth and high-speed communication possibility using optical fibers is highly interesting. For single wavelength communication, dispersion shifted fiber is enough. But for applications such as DWDM this method can not provide high-speed possibility. In these applications, the physical media should provide the flat, minimum, and uniform dispersion as well as dispersion slope ideally. Also, in the case of flat dispersion characteristic, nonlinear effects such as Four Wave Mixing (FWM) do not restrict the bandwidth of the fiber and the number of channels in DWDM applications due to phase mismatching.

There are some interesting reported papers, which we are going to review some of them and present their limitations for the proposed purposes.

As a first and interesting work, we can point out to paper published by R. Varshney et al. [1]. In this paper a flat optical fiber is presented to minimize dispersion and its slope. In this design, core radius, effective area, and carrier wavelength are 1 μm, 56.1 μm^2 and 1.55 μm respectively. According to their calculations, the dispersion duration is [2.7–3.4] ps/Km/nm within [1.53–1.61] μm interval and

the dispersion slope is 0.01 ps/Km/nm^2 at 1.55 µm wavelength. The presented paper introduces 80 nm bandwidth that is small for today DWDM applications which includes only C and L bands for data transmission.

A second work reported by Tian et al. [2] discusses about the effective area increasing for RI and RII triple-clad optical fibers. The reported dispersion and dispersion slope at [1.54–1.62] µm wavelength duration are 4.5 ps/Km/nm and 0.006 ps/Km/nm^2 respectively. The proposed design has small bandwidth for DWDM applications and is not so small for high-speed data transmission.

There are other papers presented to minimize dispersion and shift the zero-dispersion wavelength to requested values [3–6]. But the obtained results do not satisfactory.

General information about physical mediums carrying information especially for coaxial and optical fibers including capabilities and limitations can be found in [7, 8].

Excess study of previous works indicates that the reported optical fibers do not have very appreciable features to communicate high performance in order to satisfy today requested demands.

For this purpose, in this paper, a design method based on the Genetic Algorithm [9] is presented to find out optimum values for each structure especially as an example for RII triple-clad optical fibers. In this case we have six optical and geometrical parameters, which must be determined for optimum operation. Details of the design procedure applied to this problem will be discussed in the subsequent sections. In order to evaluate the propagation characteristics, the Transfer Matrix Method (TMM) [10, 11] is developed in cylindrical coordinate. In the suggested design technique, two interesting fitness functions have proposed to minimize the pulse broadening factor [12] (small dispersion as well as dispersion slope) and maximize the bandwidth (wavelength duration between zeros of the dispersion curve) as well as dispersion be lower than a threshold. Also, in these situations, nonlinear effects can limit the propagation performance that discussed something about in [13].

The paper organization is as follows.

The modal analysis based on cylindrical TMM method is presented in Section 2. Section 3 includes the Dispersion and dispersion slope analysis. Then In Section 4, we introduce the optimization technique and give design guidelines for achieving the desired performance. In the following, simulation results will be discussed for validating our suggested process. Finally the paper ends with a short conclusion.

2. MODAL ANALYSIS USING CYLINDRICAL TMM

In this section, the modal analysis based on cylindrical TMM for the proposed structure illustrated in Fig. 1 is presented.

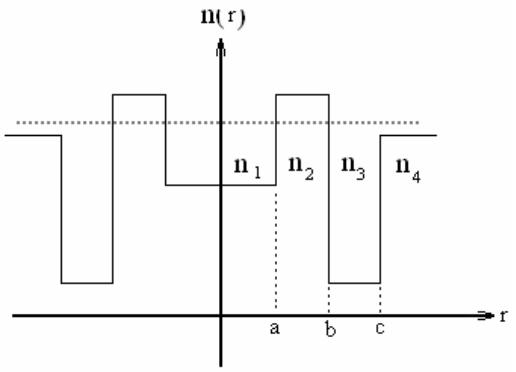

Figure 1. The refractive index profile of the proposed structures (RII).

For this structure the refractive index is defined as follows.

$$n(r) = \begin{cases} n_1, & 0 < r < a, \\ n_2, & a < r < b, \\ n_3, & b < r < c, \\ n_4, & c < r, \end{cases} \tag{1}$$

where r is the radius position of optical fiber. It is well known that the effective refractive index is given by $n_{eff} = \beta/k_0$, where β is the propagation wave vector of guided modes and k_0 is the wave number in vacuum. Based on the effective refractive index, the operation range of the proposed structure (RII) can be defined as $n_4 < n_{eff} < n_2$.

According to the following TMM approach, field distribution and guided modes conditions are demonstrated. For this purpose, the following approximation for the optical fiber refractive index is done and the TMM approach can be developed as follows (Fig. 2).

By using the Maxwell equations, LP approximation ($E_x = 0$, $H_y \approx 0$ and electric field is polarized in Y-direction) and the staircase approximated refractive index, the fields distribution in ith layer can be expressed as follows.

$$\begin{bmatrix} jE_z \\ E_y \end{bmatrix}_{r=a_i} = U \begin{bmatrix} d_{11} & d_{12} \\ d_{21} & d_{22} \end{bmatrix} \begin{bmatrix} A_i \\ B_i \end{bmatrix}, \tag{2}$$

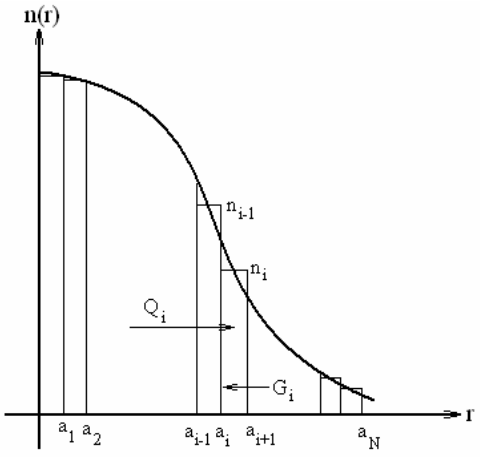

Figure 2. Staircase approximation of the refractive index for developing TMM method.

where $U = e^{[j(\omega t-\beta z)]}$ is fast varying part of field distribution. Also, for $n_i k_0 > \beta$ and $n_i k_0 < \beta$, matrix elements are defined as follows.

$$\begin{aligned} &n_i k_0 > \beta \\ &d_{11} = -\left(\kappa_i/2\beta\right)\left[J_{l+1}(\kappa_i r)\sin\left(l+1\right)\theta + J_{l-1}(\kappa_i r)\sin\left(l-1\right)\theta\right], \\ &d_{12} = -\left(\kappa_i/2\beta\right)\left[N_{l+1}(\kappa_i r)\sin\left(l+1\right)\theta + N_{l-1}(\kappa_i r)\sin\left(l-1\right)\theta\right], \\ &d_{21} = J_l(\kappa_i r)\cos l\theta, \quad d_{22} = N_l(\kappa_i r)\cos l\theta, \end{aligned} \tag{3}$$

where $\kappa_i = (n_i^2 k_0^2 - \beta^2)^{1/2}$, $k_0 = 2\pi/\lambda$, J_l and N_l are first and second order Bessel functions respectively.

$$\begin{aligned} &\beta > n_i k_0 \\ &d_{11} = -\left(\gamma_i/2\beta\right)\left[K_{l+1}(\gamma_i r)\sin\left(l+1\right)\theta - K_{l-1}(\gamma_i r)\sin\left(l-1\right)\theta\right], \\ &d_{12} = \left(\gamma_i/2\beta\right)\left[I_{l+1}(\gamma_i r)\sin\left(l+1\right)\theta - I_{l-1}(\gamma_i r)\sin\left(l-1\right)\theta\right], \\ &d_{21} = K_l(\gamma_i r)\cos l\theta, \quad d_{22} = I_l(\gamma_i r)\cos l\theta, \end{aligned} \tag{4}$$

where $\gamma_i = (\beta^2 - k_0^2 n_i^2)^{1/2}$, I_l and K_l are first and second order Modified Bessel functions respectively. Since above obtained relations are correct for all values of θ, but for absence of complication and easy mathematical calculations, we assume a special value for θ, for simplification of the reported mathematical relations, such that $\sin(l-1)\theta = 0$, $\sin(l+1)\theta \neq 0$, $\cos l\theta \neq 0$. So, based on this assumption,

Eq. (2) can be converted to the following simple case.

$$n_i k_0 > \beta$$
$$\left[\begin{array}{c} \tilde{E}_z \\ \tilde{E}_y \end{array}\right]_{r=a_i} = U \left[\begin{array}{cc} \kappa_i J_{l+1}(\kappa_i r)/\beta & \kappa_i N_{l+1}(\kappa_i r)/\beta \\ -J_l(\kappa_i r) & -N_l(\kappa_i r) \end{array}\right] \left[\begin{array}{c} A_i \\ B_i \end{array}\right], \quad (5)$$

where new variables are defined as follows.

$$\tilde{E}_z = -\left[2/\sin\left(l+1\right)\theta\right] jE_z, \quad (6)$$
$$\tilde{E}_y = -\left[1/\cos\left(l\theta\right)\right] E_y. \quad (7)$$
$$\beta > n_i k_0$$
$$\left[\begin{array}{c} \tilde{E}_z \\ \tilde{E}_y \end{array}\right]_{r=a_i} = U \left[\begin{array}{cc} \gamma_i K_{l+1}(\gamma_i r)/\beta & \gamma_i I_{l+1}(\gamma_i r)/\beta \\ -K_l(\gamma_i r) & -L_l(\gamma_i r) \end{array}\right] \left[\begin{array}{c} A_i \\ B_i \end{array}\right]. \quad (8)$$

For concluding fields distribution based on TMM approach, we need the propagation and dynamic matrices. First the propagation matrix based on field distribution inside each layer is considered. Then dynamic matrix is concentrated. Now, by using variables defined in Eqs. (6) and (7) the propagation matrix for ith layer is expressed in the following.

$$\left[\begin{array}{c} \tilde{E}_z \\ \tilde{E}_y \end{array}\right]_{r=r_2} = Q_i \left[\begin{array}{c} \tilde{E}_z \\ \tilde{E}_y \end{array}\right]_{r=r_1} = \left[\begin{array}{cc} q_{11} & q_{12} \\ q_{21} & q_{22} \end{array}\right] \left[\begin{array}{c} \tilde{E}_z \\ \tilde{E}_y \end{array}\right]_{r=r_1}, \quad (9)$$
$$a_i \le r_1,\ r_2 \le a_{i+1}.$$

where the matrix elements using Lommel's function for two separate cases are obtained as follows.

$n_i k_0 > \beta$,

$$\begin{aligned} q_{11} &= \left(\frac{\pi\kappa_i r_1}{2}\right)\left[J_{l+1}(\kappa_i r_2)N_l\left(\kappa_i r_1\right) - J_l\left(\kappa_i r_1\right)N_{l+1}\left(\kappa_i r_2\right)\right], \\ q_{12} &= \left(\frac{\pi\kappa_i^2 r_1}{2\beta}\right)\left[J_{l+1}\left(\kappa_i r_2\right)N_{l+1}\left(\kappa_i r_1\right) - J_{l+1}\left(\kappa_i r_1\right)N_{l+1}\left(\kappa_i r_2\right)\right], \\ q_{21} &= -\left(\frac{\pi\beta r_1}{2}\right)\left[J_l\left(\kappa_i r_2\right)N_l\left(\kappa_i r_1\right) - J_l\left(\kappa_i r_1\right)N_l\left(\kappa_i r_2\right)\right], \\ q_{22} &= -\left(\frac{\pi\kappa_i r_1}{2}\right)\left[J_l\left(\kappa_i r_2\right)N_{l+1}\left(\kappa_i r_1\right) - J_{l+1}\left(\kappa_i r_1\right)N_l\left(\kappa_i r_2\right)\right]. \end{aligned} \quad (10)$$

Also, for $\beta > n_i k_0$ the following relations can be obtained.

$$\begin{aligned} q_{11} &= (\gamma_i r_1)\left[I_{l+1}(\gamma_i r_2)K_l(\gamma_i r_1) + I_l(\gamma_i r_1)K_{l+1}(\gamma_i r_2)\right], \\ q_{12} &= \left(\frac{\gamma_i^2 r_1}{\beta}\right)\left[I_{l+1}(\gamma_i r_2)K_{l+1}(\gamma_i r_1) - I_{l+1}(\gamma_i r_1)K_{l+1}(\gamma_i r_2)\right], \\ q_{21} &= (\beta r_1)\left[I_l(\gamma_i r_2)K_l(\gamma_i r_1) - I_l(\gamma_i r_1)K_l(\gamma_i r_2)\right], \\ q_{22} &= (\gamma_i r_1)\left[I_l(\gamma_i r_2)K_{l+1}(\gamma_i r_1) + I_{l+1}(\gamma_i r_1)K_l(\gamma_i r_2)\right]. \end{aligned} \tag{11}$$

After developing the propagation matrix, one can develop dynamic matrix based on boundary condition in interface between adjacent layers, which is illustrated in Eq. (12).

$$\begin{bmatrix} \tilde{E}_z \\ \tilde{E}_y \end{bmatrix}_{r=a_i^+} = G_i \begin{bmatrix} \tilde{E}_z \\ \tilde{E}_y \end{bmatrix}_{r=a_i^-}, \quad G_i = \begin{bmatrix} 1 & 0 \\ 0 & (n_{i-1}/n_i)^2 \end{bmatrix}. \tag{12}$$

Now using Eq. (9) and Eq. (12), field distribution inside stack of multilayer is given as follows.

$$\begin{bmatrix} \tilde{E}_z \\ \tilde{E}_y \end{bmatrix}_{r=a_N} = M \begin{bmatrix} \tilde{E}_z \\ \tilde{E}_y \end{bmatrix}_{r=a_1} = \begin{bmatrix} m_{11} & m_{12} \\ m_{21} & m_{22} \end{bmatrix} \begin{bmatrix} \tilde{E}_z \\ \tilde{E}_y \end{bmatrix}_{r=a_1}, \tag{13}$$

where $M = G_N \prod_{i=1}^{N-1} (Q_{N-i} \cdot G_{N-i})$.

In order to present a strict algorithm for obtaining the wave vectors of the guided modes, it is assumed that n_0 and n_e are the refractive index of the first and last layers respectively. According to established method for field distribution, the following relations show the matrix form of the electric fields.

$$\beta < n_0 k_0$$

$$\begin{bmatrix} \tilde{E}_z \\ \tilde{E}_y \end{bmatrix}_{r=a_1} = U \begin{bmatrix} -\kappa_0 J_{l+1}(\kappa_0 a_1)/\beta \\ -J_l(\kappa_0 a_1) \end{bmatrix} A_1, \tag{14a}$$

$$\beta > n_0 k_0$$

$$\begin{bmatrix} \tilde{E}_z \\ \tilde{E}_y \end{bmatrix}_{r=a_1} = U \begin{bmatrix} -\gamma_0 I_{l+1}(\gamma_0 a_1)/\beta \\ -I_l(\gamma_0 a_1) \end{bmatrix} B_1. \tag{14b}$$

In the case of last layer, it will be defined as follow.

$$\begin{bmatrix} \tilde{E}_z \\ \tilde{E}_y \end{bmatrix}_{r=a_N} = U \begin{bmatrix} \gamma_e K_{l+1}(\gamma_e a_N)/\beta \\ -K_l(\gamma_e a_N) \end{bmatrix} A_e \tag{14c}$$

According to Eq. (14), depends on the guided wave vector value, one of the following two matrixes illustrate the characteristic equation of

the proposed structure. Then zeros of the following determinants give guided modes.

$$\beta < n_0 k_0$$
$$\begin{bmatrix} K_l(\gamma_e a_N) & m_{21}\kappa_0 J_{l+1}(\kappa_0 a_1)/\beta - m_{22} J_l(\kappa_0 a_1) \\ -\gamma_e K_{l+1}(\gamma_e a_N)/\beta & m_{11}\kappa_0 J_{l+1}(\kappa_0 a_1)/\beta - m_{12} J_l(\kappa_0 a_1) \end{bmatrix} \begin{bmatrix} A_1 \\ A_e \end{bmatrix} = 0, \tag{14d}$$

$$\beta > n_0 k_0$$
$$\begin{bmatrix} m_{11}\gamma_0 I_{l+1}(\gamma_0 a_1)/\beta + m_{12} I_l(\gamma_0 a_1) & \gamma_e K_{l+1}(\gamma_e a_N) \\ m_{21}\gamma_0 I_{l+1}(\gamma_0 a_1)/\beta + m_{22} I_l(\gamma_0 a_1) & -K_l(\gamma_e a_N) \end{bmatrix} \begin{bmatrix} B_1 \\ A_e \end{bmatrix} = 0. \tag{14e}$$

As another alternative under the LP approximation, the guided modes and propagation wave vectors can be evaluated by using a determinant which is constructed by the boundary conditions.

$$\begin{vmatrix} I_m(W_1) & -J_m(U_2) & -Y_m(U_2) \\ 0 & J_m(\overline{U_2}) & Y_m(\overline{U_2}) \\ 0 & 0 & 0 \\ W_1 I'_m(W_1) & -U_2 J'_m(U_2) & -U_2 Y'_m(U_2) \\ 0 & \overline{U_2} J'_m(\overline{U_2}) & \overline{U_2} Y'_m(\overline{U_2}) \\ 0 & 0 & 0 \\ 0 & 0 & 0 \\ -I_m(W_3) & -K_m(W_3) & 0 \\ I_m(\overline{W_3}) & K_m(\overline{W_3}) & -K_m(W_4) \\ 0 & 0 & 0 \\ -W_3 I'_m(W_3) & -W_3 K'_m(W_3) & 0 \\ \overline{W_3} I'_m(\overline{W_3}) & \overline{W_3} K'_m(\overline{W_3}) & -W_4 K'_m(W_4) \end{vmatrix} = 0,$$
$$(n_4 < n_e < n_2), \tag{15}$$

where the appeared transversal propagation constants are defined as follows. It should be mentioned that for extracting guided wave vectors the Newton-Ralfson and Bisection methods are used.

$$\begin{aligned} &U_2 = a\sqrt{k_0^2 n_2^2 - \beta^2}, \quad \overline{U_2} = \frac{P}{Q} U_2, \\ &W_1 = a\sqrt{\beta^2 - k_0^2 n_1^2}, \quad W_3 = b\sqrt{\beta^2 - k_0^2 n_3^2}, \\ &\overline{W_3} = \frac{1}{P} W_3, \quad W_4 = c\sqrt{\beta^2 - k_0^2 n_4^2}, \end{aligned} \tag{16}$$

where $P = \frac{b}{c}$ and $Q = \frac{a}{c}$ are constants.

3. THEORETICAL ANALYSIS OF DISPERSION AND DISPERSION SLOPE

In this section dispersion and dispersion slope analysis based on derived relations in previous section including waveguide and material dispersions (single mode fibers) are done. For the proposed optical fiber, the optical parameters are defined as follows.

$$R_1 = \frac{n_2 - n_3}{n_2 - n_1}, \quad R_2 = \frac{n_1 - n_4}{n_2 - n_1}. \tag{17}$$

Also, we define the relative index difference as follows.

$$\Delta = \frac{n_2^2 - n_4^2}{2n_4^2} \approx \frac{n_2 - n_4}{n_4}. \tag{18}$$

Finally, the normalized frequency and propagation parameters are defined as follows.

$$V = k_0 a \sqrt{n_2^2 - n_4^2} \tag{19}$$

$$B = \frac{(\beta/k_0)^2 - n_4^2}{n_2^2 - n_4^2} = 1 - \left(\frac{U_2}{V}\right)^2 \tag{20}$$

Now, using the defined parameters and derived relations in previous section, the total dispersion as well as dispersion slope relations for the introduced single mode fiber are as follows.

$$D = -\frac{\lambda}{c}\frac{d^2 n_4}{d\lambda^2}\left[1 + \Delta\frac{d(VB)}{dV}\right] - \frac{N_4}{c}\frac{\Delta}{\lambda}V\frac{d^2(VB)}{dV^2}, \tag{21}$$

$$S = -\frac{\lambda}{c}\frac{d^3 n_4}{d\lambda^3}\left[1 + \Delta\frac{d(VB)}{dV}\right] - \frac{1}{c}\frac{d^2 n_4}{d\lambda^2}\left[1 + \Delta\frac{d(VB)}{dV}\right] + \frac{N_4}{c}\left(\frac{\Delta}{\lambda^2}\right)V^2\frac{d^3(VB)}{dV^3} + 2\frac{N_4}{c}\frac{\Delta}{\lambda^2}V\frac{d^2(VB)}{dV^2} + 2\frac{\Delta}{c}\frac{d^2 n_4}{d\lambda^2}V\frac{d^2(VB)}{dV^2}, \tag{22}$$

where $N_4 = n_4 - \lambda(dn_4/d\lambda)$ is the group index of the outer cladding layer. Also, the Sellmeier formula can be used for calculation of material dispersion ($dn_4/d\lambda$ and $d^2n_4/d\lambda^2$). For complete calculation of Eq. (21) and Eq. (22), $d(VB)/dV$, $Vd^2(VB)/dV^2$, and $V^2d^3(VB)/dV^3$ must be calculated.

For this purpose Eq. (16) and the following equations can be used.

$$\frac{d(VB)}{dV} = 1 + \left(\frac{U_2}{V}\right)^2\left(1 - 2\frac{V}{U_2}\frac{dU_2}{dV}\right), \tag{23}$$

$$V\frac{d^2(VB)}{dV^2} = -2\left(\frac{dU_2}{dV} - \frac{U_2}{V}\right)^2 - 2U_2\frac{d^2U_2}{dV^2}, \quad (24)$$

$$V^2\frac{d^3(VB)}{dV^3} = 6\left(\frac{dU_2}{dV} - \frac{U_2}{V}\right)^2 - 2U_2V\frac{d^3U_2}{dV^3} - 6V\frac{d^2U_2}{dV^2}\left(\frac{dU_2}{dV} - \frac{U_2}{V}\right), \quad (25)$$

To complete calculation of total dispersion and dispersion slope, estimation of Eq. (23), Eq. (24) and Eq. (25) are necessary. For this purpose, the essential calculations of U_2 and it derivatives are necessary in this step. To obtain the dispersion and its slope, relationships are done according to the method introduced and explained completely in Ref. [14]. Due to analytically based relationships, this approach accurately covers all the numerical methods reported so far.

4. OPTIMIZATION TECHNIQUE USING GENETIC ALGORITHM

As said in the introduction, in this paper we attempt to present an optimized RII triple-clad optical fiber for obtaining good performance from bandwidth, dispersion and dispersion slope points of view. The optimization technique is based on the Genetic Algorithm (GA). A GA belongs to a class of evolutionary computation techniques [9] based on models of biological evolution. These methods have proved useful in domains that are not well understood or for search spaces, which are too large to be efficiently searched by standard methods. To express the fiber optic structure we consider three optical and three geometrical parameters. According to the GA technique, the problem will have six genes which explain those parameters. It should be mentioned that the initial range of parameters are chosen after some conceptual examinations. The initial population has fifty chromosomes which cover the search space approximately. By using the initial population, the dispersion (β_2) and dispersion slope (β_3) which are the important factors in the following related fitness function can be calculated. Consequently elites are selected to survive in the next generation. This algorithm is repeated some time and the optical and geometrical parameters corresponding to the minimum fitness function value are extracted. Eq. (26) shows our proposal for fitness function of pulse broadening factor.

$$F_{BF} = \sum_{\lambda}\sum_{Z}\left[\left(1+\frac{C\beta_2(\lambda)Z}{t_i^2}\right)^2 + \left(\frac{\beta_2(\lambda)Z}{t_i^2}\right)^2 + (1+C^2)^2\left(\frac{\beta_3(\lambda)Z}{2t_i^3}\right)^2\right]^{\frac{1}{2}}, \quad (26)$$

where F_{BF}, C, β_2, t_i, λ, Z, and β_3 are broadening factor, chirp parameter, second derivative of the guided wave vector, initial full width at half maximum of input pulse, wavelength, distance, and third derivative of the guided wave vector respectively. Applying this proposed fitness function, the dispersion and dispersion slope are minimized simultaneously. Therefore, this condition is corresponded to maximum value for dispersion length. In the following mathematical relations for β_2, β_3 and (dispersion length) L_D are given.

$$\beta_2 = \frac{d^2}{d\omega^2}\beta(\omega)|_{\omega=\omega_c},\ \beta_3 = \frac{d^3}{d\omega^3}\beta(\omega)|_{\omega=\omega_c} = \left(S - \frac{4\pi c}{\lambda^3}\beta_2\right)\frac{\lambda^4}{(2\pi c)^2}, \quad (27)$$

$$L_D = \frac{t_i^2}{|\beta_2|}. \quad (28)$$

Meanwhile, in order to maximize the bandwidth of the dispersion curve, the following fitness function is introduced.

$$F_{BW} = |\lambda_2 - \lambda_1|, \quad D(\lambda_{1,2}) = 0, \quad (29)$$

where F_{BW} is the dispersion bandwidth of the proposed structure and $\lambda_{1,2}$ are corresponding to the zero dispersion wavelengths. Also, in this fitness function another limitation is applied on software in order to limit the dispersion value lower than a predefined measure.

The flowchart given in Fig. 3 explains the foregoing design strategy clearly.

In the next section, our proposed fitness functions and GA optimization method are used for investigation of the proposed structure and simulated results are discussed.

5. RESULTS AND DISCUSSION

In this section, based on the developed design method, simulation results are presented. The designed structures related to the first (F_{BF}) and second (F_{BW}) fitness functions are named optimized and modified cases respectively. In order to evaluate the efficiency of the design procedure, propagation characteristics are compared with the common designed structure reported in [2]. In first step, the dispersion is considered. By applying two fitness functions, the broadening factor is minimized and bandwidth of dispersion curve (the wavelengths duration between two zero dispersion wavelengths) is maximized. In this simulation the following durations for simulation parameters are assumed.

According to the illustrated curves in Fig. 4, bandwidth for common case (Ref. [2]) is about 200 nm within the wavelength duration

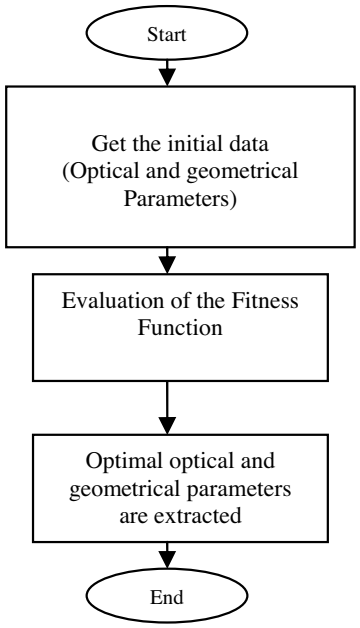

Figure 3. The scheme of the design procedure.

of [1.45–1.65] μm, whereas this quantity is 230 nm for modified case within [1.42–1.65] μm duration which is equivalent to 15% increase in the bandwidth. Also, maximum dispersion for common case is 3.7 ps/Km/nm, whereas dispersion for modified and optimized cases are 3 ps/Km/nm and 2.02 ps/Km/nm respectively. The last case is

Table 1. Initial population ranges and values for the designed optical fiber structure.

Parameters	Duration	Optimized Value	Modified Value	Common Value [2]
R_1	[1.2–5.2]	1.2786	1.2786	2
R_2	[(−0.5)–(−0.05)]	−0.3818	−0.0553	−0.1
Δ	[0.003–0.01]	7.908×10^{-3}	4.488×10^{-3}	5.9×10^{-3}
P	[0.5–0.8]	0.6382	0.5148	0.7
Q	[0.1–0.42]	0.3327	0.3128	0.4
a	[2.2–2.8] μm	2.3092 μm	2.4393 μm	2.6 μm

equivalent to about 46% decrease in dispersion compared to common case.

Also, the proposed design method based on the F_{BF} fitness function can be used to shift the zero dispersion wavelength to the arbitrary requested wavelength. It should be mentioned that in this case the first summation on wavelengths must be replaced to only one wavelength that is equal to the requested zero dispersion wavelength. For illustration of this ability of the proposed algorithm, we assumed 1.55 µm for the zero dispersion wavelength and optimized curve is corresponds to this wavelength and illustrated in Fig. 4. So, the proposed idea is excellent for design of optical fibers suitable in broadband optical communications such as DWDM and OTDM applications. In the following, the dispersion slope of common, optimized and modified cases are illustrated in Fig. 5. It is obvious that the optimized and modified cases have wide bandwidths as well as more uniformity compared to common case. For excess clarification, Table 2 is given to show the slope of dispersion slope in the S, C and L communication bands.

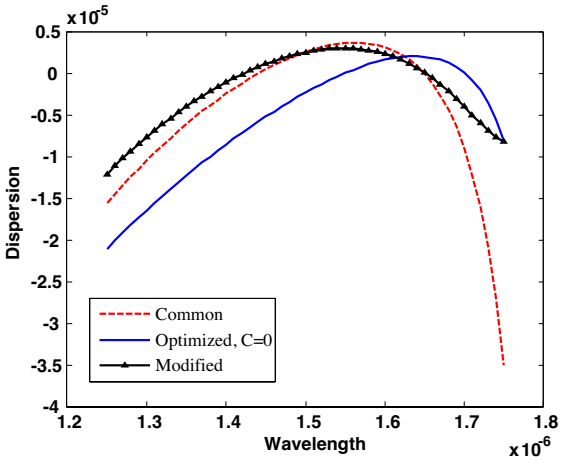

Figure 4. Dispersion (s/m^2) vs. wavelength (m) for common case [2], optimized case using F_{BF} fitness function (at 1.55 µm), and modified case using F_{BW} fitness function.

It is clear that the slope of dispersion slope in optimized case is about half of common case. So, as a result one can imagine that pulse broadening for optimized case is smaller than common case. Also, it is shown that the modified case is excellent for C-band compared to the two other cases. Generally in wide bandwidth ranges optimized

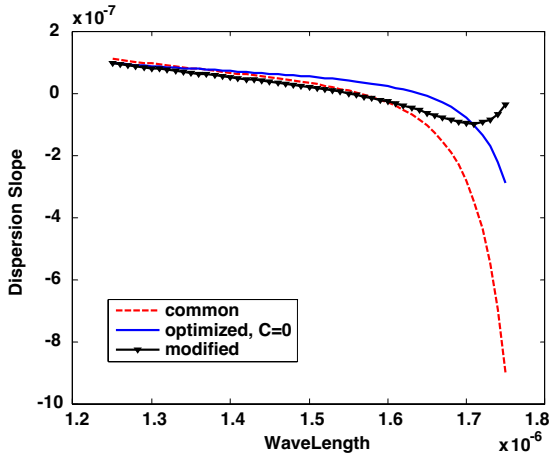

Figure 5. Dispersion slope (s/m^3) vs. wavelength for common, optimized and modified cases (normalized to 10^{-9}).

Table 2. Slope of dispersion slope in S, C and L bands.

Band	Slope of Dispersion Slope for Optimized Case	Slope of Dispersion Slope for Common Case	Slope of Dispersion Slope for Modified Case
S (1500 nm)	−0.214	−0.399	−0.3660
C (1550 nm)	−0.298	−0.5964	−0.1820
L (1600 nm)	−0.462	−1.03	−0.64

case is better for small pulse broadening purposes. Consequently, it is excellent for dense wavelength division multiplexing (DWDM) application.

Thus, owing to discussion presented earlier, the optimized case is selected and its other propagation features are evaluated. Fig. 6 illustrates the pulse broadening factor at the zero dispersion wavelength (1.55 μm) versus distance for Gaussian input pulse with 5 psec Full-width at half maximum. It is evident that the broadening factor just increase to 1.0016 after 200 Km propagation that is excellent for practical case. In other words, after 200 Km traveling only 0.16% increase in broadening factor is observed. It is remarkable that the broadening factor increase to 1.2794 in the common case structure at

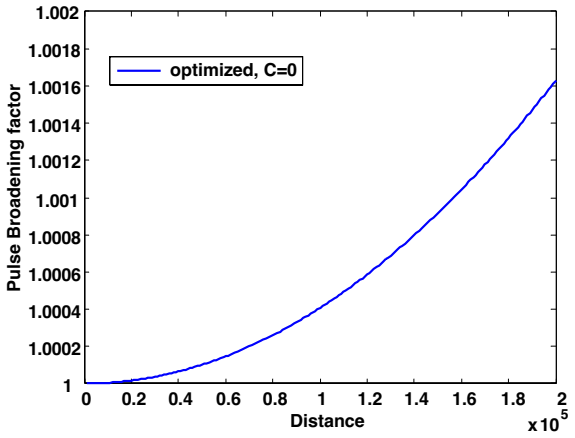

Figure 6. Pulse broadening factor vs. distance (m) for zero dispersion wavelength (1.55 μm).

1.44 μm which is related to 27.94% growth in this factor.

Furthermore, in order to show the excellent feature of proposed optimized case, the pulse broadening factor is computed at the wavelength about 10 nm away from the zero dispersion wavelength. The simulation outcomes show that the broadening factor increases to 1.0016 at 1.56 μm which is as same as its value at the zero dispersion wavelength. But in the common case structure and under putting forward condition, the pulse broadening factor growth is obvious at 1.45 μm and reaches to 3.975 after 200 Km propagation.

In order to illustrate the importance of the obtained small pulse broadening in the optimized case in comparison with the common one, the dispersion length of these cases are calculated and illustrated in Figs. 7 and 8.

Figure 7 shows the dispersion length of the common case. In this figure, two peaks are appeared at 1.44 μm and 1.65 μm which are related to nearly 500 Km and 900 Km of dispersion length respectively. It is useful to notice that 1.44 μm is corresponded to the zero dispersion wavelength. A similar situation is illustrated for optimized case in Fig. 8. In this figure there are two considerable dispersion lengths that are 17400 Km and 4490 Km corresponding to 1.55 μm and 1.7 μm respectively. The first peak is observed at zero-dispersion wavelength. Based on these simulations at zero-dispersion wavelengths the optimized case has 17400 Km whereas common case has 500 Km dispersion lengths that is a huge increase in the optimized case. This is equivalent to 34.8 times increase in dispersion length at the zero

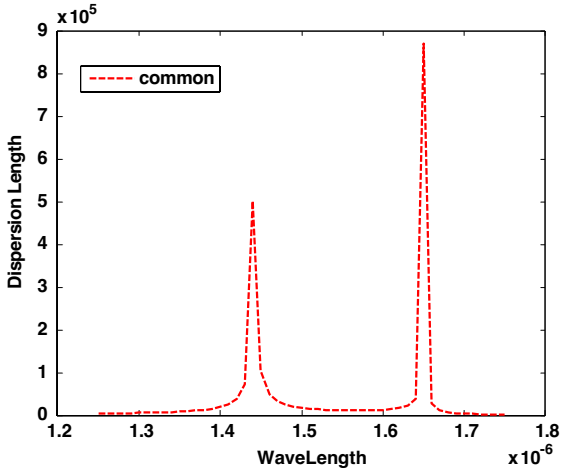

Figure 7. Dispersion length for common case.

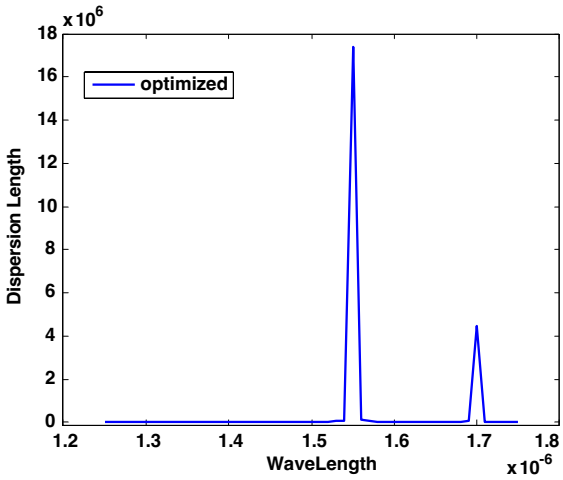

Figure 8. Dispersion length for optimized case.

dispersion wavelengths near to minimum fiber loss. Even for comparing the maximum reported dispersion lengths for both two cases, we observed that the optimized case is 19.33 times better than common case.

In the following, the bit rate is calculated at near zero dispersion wavelengths (about 40 nm away from zero dispersion wavelengths) for optimized and common cases and illustrated in Fig. 9. It is found out that the bit rates are 197.8 Gb/sec and 78.8 Gb/sec for optimized and

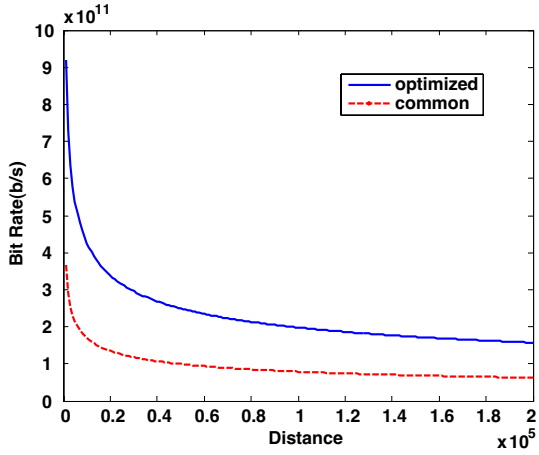

Figure 9. Bit rate vs. distance for optimized and common cases at near zero dispersion wavelengths (about 40 nm away from zero dispersion wavelengths).

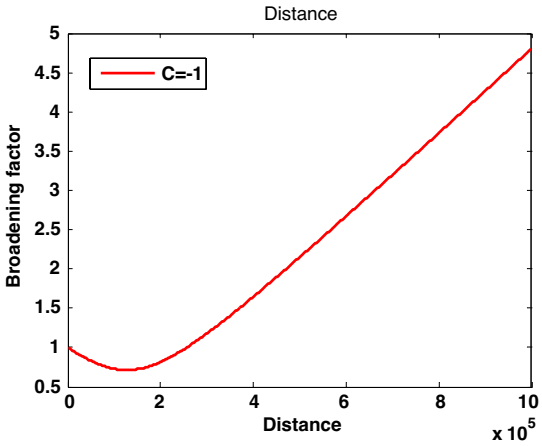

Figure 10. Pulse broadening factor vs. distance (m) for the chirped pulse case at zero-dispersion wavelength (1.55 µm).

common cases respectively at 100 Km. The bit rate in the optimized case is 2.5 times higher than common case.

In this section, the optimized case name optical fiber (RII) were investigated from many aspects such as dispersion, dispersion slope, dispersion length and bit rate points of view. It was shown that the small pulse broadening factor and large dispersion length as well as

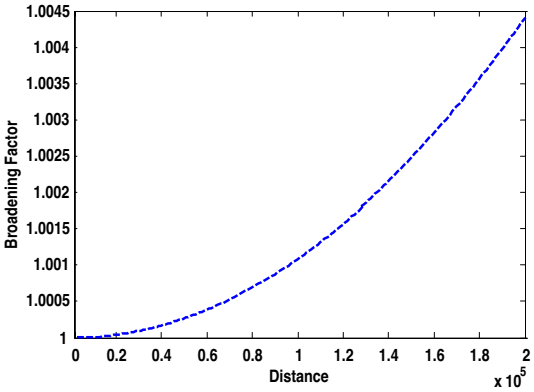

Figure 11. Pulse broadening factor vs. distance (m) for designed case over [1.52–1.58] μm wavelength duration at the zero dispersion wavelength (1.53 μm).

large bandwidth are the main advantages of the proposed optimized case structure, making it an ideal candidate for performing large bandwidth and high speed optical communication applications.

In the following we consider the chirped Gaussian pulse as an input and design an optical fiber structure by applying suggested procedure by F_{BF} as a fitness function. In simulation we set the chirp parameter to $C = -1$ and the pulse broadening versus distance is illustrated at zero dispersion wavelength in Fig. 10. After 257.2 Km propagation the output pulse width is equal to start point pulse width and the increased to 4.8027 after 1000 Km. The situation for common case is a little different and pulse width after 1000 Km traveling broadened to 5.001. The structural parameters of the proposed case with chirped Gaussian pulse as an input are given in Table 3.

With compared to Table 1, we find out that the considerable difference between parameters in these two table is related to Δ.

It is noticeable that the suggested F_{BF} fitness function could applied to the large wavelength interval instead of predefined single wavelength. In the case of single wavelength, the zero dispersion wavelength is led to the predefined value. But in the duration ones, there is no precise prediction about the zero dispersion wavelength value. Fig. 11 demonstrates the pulse broadening factor for the situation which the F_{BF} is used at [1.52–1.58] μm interval. In other word, it is attempted to minimize the pulse broadening factor in the given wavelengths. It is observed that the zero dispersion wavelength is equal to 1.53 μm and the pulse broadening factor reaches to 1.0044 after 200 Km propagation.

Table 3. Structural parameters value for the proposed optical fiber structure with chirped input pulse.

Parameter	Repotred Value for Chirped Pulse case
R_1	1.2786
R_2	-0.3872
Δ	9.5067×10^{-3}
P	0.6382
Q	0.3327
a	2.3092 μm

6. CONCLUSION

By applying the introduced design method, the optimized RII triple-clad optical fiber is reported. It is shown that the obtained optimized case introduces so interesting features to be used for optical communication. We show that this structure have 17400 Km dispersion length, 1.0016 pulse broadening factor after 200 Km, and 197.8 Gb/sec at 100 Km. Based on these reported results the introduced fiber illustrate good performance for high speed data transmission lines and especially OTDM applications. Also, this methodology is capable to shift the zero dispersion wavelength to an arbitrary requested wavelength and introduce possible minimum dispersion slope. In the simulated results, we discovered that Δ is critical parameter in the optimization procedure for changing input pulse from chirped to without chirping. Finally, the F_{BF} introduced fitness function let the pulse broadening factor minimize within a duration of wavelengths that is so important for large bandwidth applications such as DWDM operation.

ACKNOWLEDGMENT

The authors would like to thank Iran telecommunication research center for providing technical and financial supports.

REFERENCES

1. Varshney, R. K., A. K. Ghatak, I. C. Goyal, and S. Antony C, "Design of a flat field fiber with very small dispersion slope,"

Optical Fiber Technology, Vol. 9, 189–198, 2003.

2. Tian, X. and X. Zhang, "Dispersion-flattened designs of the large effective-area single-mode fibers with ring index profiles," *Optics Communications*, Vol. 230, 105–113, 2004.
3. Zhang, X. and X. Tian, "Analysis of waveguide dispersion characteristics of WI- and WII-type triple-clad single-mode fibers," *Optics & Laser Technology*, Vol. 35, 237–244, 2003.
4. Kato, T., M. Hirano, A. Tada, K. Fokuada, T. Fujii, T. Ooishi, Y. Yokoyama, M. Yoshida, and M. Onishi, "Dispersion flattened transmission line consisting of wide-band non-zero dispersion shifted fiber and dispersion compensating fiber module," *Optical Fiber Technology*, Vol. 8, 231–239, 2002.
5. Agrawal, G. P., *Fiber-optic Communication Systems*, 3rd edition, John Wiley & Sons, 2002.
6. Zhang, X. and X. Wang, "The study of chromatic dispersion and chromatic dispersion slope of WI- and WII-type triple-clad single-mode fibers," *Optics & Laser Technology*, Vol. 37, 167–172, 2005.
7. Ghatak, A. and K. Thyagarajan, *Introduction to Fiber Optics*, Cambridge University Press, 2002.
8. Nunes, F. D. and C. A. de Souza Melo, "Theoretical study of coaxial fibers," *Applied Optics*, Vol. 35, 388–398, 1996.
9. Goldberg, D. E., *Genetic Algorithms in Search, Optimization and Machine Learning*, Addison-Wesley, Reading, 1989.
10. Sakai, J.-I. and T. Kimura, "Bending loss of propagation in arbitrary-index profile optical fibers," *Applied Optics*, Vol. 17, No. 10, 1978.
11. Yeh, P., *Optical Waves in Layered Media*, John Wiley & Sons, New York, 1988.
12. Zhang, X., L. Xie, X. Tian, and S. Hou, "Chirped Gaussian pulse broadening induced by chromatic dispersion in the triple-clad single-mode fiber with a depressed index inner cladding," *Optical Fiber Technology*, Vol. 10, 215–231, 2004.
13. Hattori, H. T. and A. Safaei-Jazi, "Fiber designs with significantly reduced nonlinearity for very long distance transmission," *Applied Optics*, Vol. 37, 3190–3197, 1998.
14. Rostami, A. and M. Savadi-Oskouei, "Investigation of dispersion characteristic in MI- and MII-type single mode optical fibers," *Optics Communications*, Vol. 271, 413–420, 2007.